A Simple Semaphore Signaling Technique for Ultra-High Frequency Spacecraft Communications

S. Butman,[1] E. Satorius,[1] and P. Ilott[1]

For planetary lander missions such as the upcoming Phoenix mission to Mars, the most challenging phase of the spacecraft-to-ground communications is during the critical phase termed entry, descent, and landing (EDL). At 8.4 GHz (X-band), the signals received by the largest Deep Space Network (DSN) antennas can be too weak for even 1 bit per second (bps) and therefore not able to communicate critical information to Earth. Fortunately, the lander's ultra-high frequency (UHF) link to an orbiting relay can meet the EDL requirements, but the data rate needs to be low enough to fit the capability of the UHF link during some or all of EDL. On Phoenix, the minimum data rate of the as-built UHF radio is 8 kbps and requires a signal level at the Odyssey orbiter of at least −120 dBm. For lower signaling levels, the effective data rate needs to be reduced, but without incurring the cost of rebuilding and requalifying the equipment. To address this scenario, a simple form of frequency-shift keying (FSK) has been devised by appropriately programming the data stream that is input to the UHF transceiver. This article describes this technique and provides performance estimates. Laboratory testing reveals that input signal levels at −140 dBm and lower can routinely be demodulated with the proposed signaling scheme, thereby providing a 20-dB and greater margin over the 8-kbps threshold.

I. Introduction

Communication during critical maneuvers is now a NASA requirement on all missions in order to learn the cause of a failure or even the loss of a mission. This vital information will be used to avoid duplication of any design flaws on future missions. Typically, planetary missions rely on the well-proven 8.4-GHz (X-band) link to the Deep Space Network (DSN). However, sometimes it is not possible to obtain an effective X-band link to the DSN from a spacecraft during entry, descent, and landing (EDL). The Phoenix mission, which is to launch in August 2007 and land near the north pole of Mars to dig for traces of water, is an example of such a case. Low X-band power (15 W), large distance from Mars (2 AU), and unpredictability of spacecraft antenna pointing during EDL made the X-band link unreliable at any useful data rate. For that reason (and other reasons concerning landed data return, mass, and cost), the project decided to remove X-band from the lander and rely solely on the lander's ultra-high frequency

[1] Flight Communications Systems Section.

The research described in this publication was carried out by the Jet Propulsion Laboratory, California Institute of Technology, under a contract with the National Aeronautics and Space Administration.

(UHF) radio to communicate via the UHF relay radios on the Mars Odyssey and Mars Reconnaissance Orbiter (MRO). X-band still is retained on the cruise stage and will be used for all critical maneuvers prior to EDL.

The orbiters are in approximately 2-hour 350-km and 300-km circular polar orbits, so they can be in contact with a lander on the surface for at most 12 minutes per pass. Due to the limited contact time, the UHF radios on Odyssey and Phoenix were designed to operate at only four data rates: 8 kilobits per second (kbps), 32 kbps, 128 kbps, and 256 kbps. However, even the 8-kbps rate may not be sufficiently low to close the Phoenix link to an orbiter right after its separation from the cruise stage. The UHF radios, or actually transceivers, use a standard residual-carrier binary phase-shift-keying (BPSK) modulation with a 60-deg modulation index. A received signal power-to-noise density ratio (P/N_0) of approximately 50 dB-Hz would be required to sustain a bit energy-to-noise spectral density ratio (E_b/N_0) of 5 to 10 dB at 8 kbps. On Odyssey, the UHF receiver carrier acquisition bandwidth is fixed at 20 kHz. Assuming a typical -170 dBm/Hz receiver noise spectral density, then a received signal level of -120 dBm at the orbiter would be required to acquire reliably. This can be difficult to achieve during early EDL due to large distance from the orbiter and to unfavorable antenna orientations (the lander separates from the cruise stage at an altitude higher than the orbiter) and dynamics (Doppler).

To overcome the data-rate constraints noted above, we have devised a simple low-rate, semaphore signaling scheme that can be used with the existing UHF BPSK modulation at any of the data rates, i.e., 8 kbps, 32 kbps, 128 kbps, or 256 kbps. The signaling scheme is implemented in software by appropriately programming the input bit stream to the UHF transceiver, which uses a residual-carrier, Manchester-encoded, BPSK modulator. The signaling scheme and performance analysis are presented in the following sections. As discussed in Section IV, laboratory testing reveals that input signal levels at -140 dBm and lower can routinely be demodulated with the proposed signaling scheme—a 20-dB (and greater) improvement over the 8-kbps threshold.

II. Low-Rate Semaphore Signaling Using Residual-Carrier BPSK

As previously noted, moderate rate (8-kbps) residual-carrier BPSK modulation (60-deg modulation index) requires a received P/N_0 in excess of 50 dB-Hz for reliable communications. However, by exploiting the Manchester encoding that is used in conjunction with residual-carrier modulation (to aid the carrier tracking loop), it is possible to generate semaphores (subcarriers) with fundamentals separated in frequency from the residual carrier by either $R_b/2$ or R_b, where R_b is the transmitted data rate. In the following, we assume the lowest possible data rate for the Phoenix mission, i.e., $R_b = 8$ kbps, although the method could be used with any of the other data rates.

The basic idea is to program the 8-kbps input data stream to the residual-carrier modulator to be either (1) an all 0's sequence for duration T s (T is the symbol rate for the signaling scheme) or (2) an alternating 0,1 sequence for T s. After Manchester encoding, these two T-second sequences translate into (1) a periodic 1,0 sequence with period matched to $1/8000 = 0.125$ ms and (2) a periodic 1,1,0,0 sequence with period matched to $2/8000 = 0.25$ ms. Thus, the all-0's input sequence produces an output harmonic line spectra (after Manchester encoding) with the fundamental frequency at 8 kHz, and the $1, 0, 1, 0, \ldots$ input sequence produces an output harmonic line spectra with the fundamental frequency at 4 kHz. A special software demodulator then is used to process this received signal and retrieve the low-rate bit stream. As described in Section III, this demodulator can use either the real-time EDL software developed for the Mars Exploration Rover (MER) EDL[2] [1] or a simple non-coherent binary frequency-shift-keyed (BFSK) demodulator.

[2] Multiple-frequency-shift keying (MFSK), used for MER EDL at X-band, was originally proposed for the cancelled Mars '01 lander by S. Butman (a version of MFSK semaphores was also used for Pathfinder [2]). Phoenix is a revamped version of the Mars '01 lander.

The received Manchester-encoded waveform is represented by

$$x(t) = \sqrt{2P} \cdot \cos(\delta \cdot s(t) + 2\pi f_c t + \phi_c) = \sqrt{2P} \cdot \left\{ \cos\delta \cdot \cos(2\pi f_c t + \phi_c) - \sin\delta \cdot s(t) \cdot \sin(2\pi f_c t + \phi_c) \right\} \quad (1)$$

where P is the total received power; δ is the modulation index (nominally $\pi/3$); f_c is the carrier frequency (possibly frequency shifted due to Doppler offsets or carrier drift); ϕ_c is the carrier phase; and $s(t) = \pm 1$ is the Manchester-encoded waveform. Since, over one BFSK symbol interval ($0 \le t \le T$), $s(t)$ is a periodic square wave with the period given by either $T_p = 1/8000$ s or $T_p = 1/4000$ s, it has the harmonic sine wave representation

$$s(t) = \frac{4}{\pi} \sum_{n=1}^{\infty} \frac{1}{2n-1} \cdot \sin\left(2\pi(2n-1)\frac{t}{T_P}\right), \quad 0 \le t \le T \quad (2)$$

Spectrally, $x(t)$ comprises discrete lines at the carrier, data-tone sidebands (on either side of the carrier line), and harmonics of the data tone. Sample spectra of $x(t)$ (over 1 BFSK symbol interval) are presented in Fig. 1, corresponding to $\delta = 60$ deg and with $T_p = 1/4000$ s and $T_p = 1/8000$ s. As is seen, all data-related spectral components are positioned symmetrically about the carrier line.

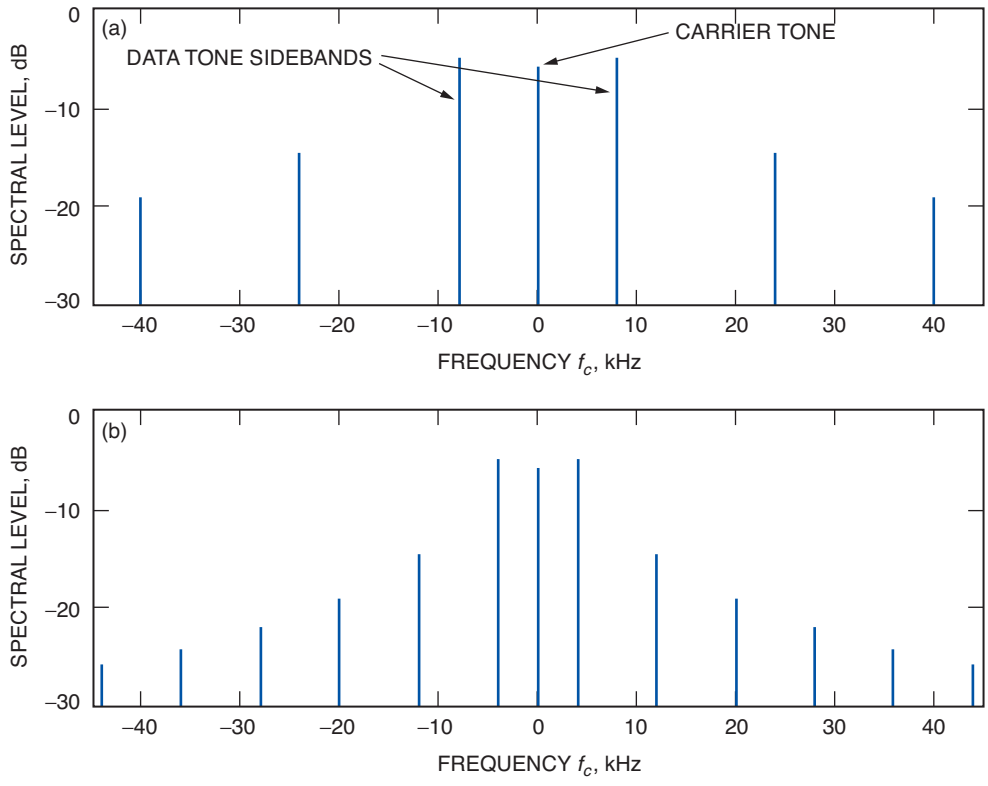

Fig. 1. Sample semaphore signal spectra over a 1-BFSK symbol interval: (a) T_p = 1/8000 s and (b) T_p = 1/4000 s.

We can express the received carrier and data powers as

$$P_c = P \cdot \cos^2 \delta \tag{3a}$$

and

$$P_d = P \cdot \sin^2 \delta \tag{3b}$$

We can further split the data power P_d into two components: (1) the power in the primary subcarrier, P_{dsc}, and (2) the power in the harmonics, P_{dh}. Thus, $P_d = P_{dsc} + P_{dh}$ or, equivalently, $P_d = P_{dsc} \cdot (1 + \rho)$, where $\rho \equiv P_{dh}/P_{dsc} = \pi^2/8 - 1$ is the ratio of harmonic-to-primary subcarrier power. Therefore, the total power in the data-tone sidebands (see Fig. 1) is given by

$$P_{dsc} = \frac{P_d}{1+\rho} = \frac{8P}{\pi^2} \cdot \sin^2 \delta \tag{4}$$

which represents about 61 percent of the total received power.

III. Demodulation of the Semaphores

A software demodulator will be used to process the semaphores. As previously noted, the demodulation of the semaphores can proceed using either the EDL multiple-frequency-shift-keyed (MFSK) tone demodulator [1] or a simple non-coherent BFSK demodulator approach. The former tracks the carrier via a fast Fourier transform (FFT) tracking algorithm (based on maximum-likelihood detection) and then detects the data tones at 4 kHz or 8 kHz via spectral folding and energy detection. The non-coherent BFSK demodulator first tracks out the carrier using a second- or third-order residual-carrier tracking loop and then detects the data tones again via spectral folding and energy detection. Given the lower-frequency dynamics at UHF (versus X-band), a third-order carrier tracking loop is sufficient to track worst-case EDL dynamics down to a received P/N_0 of less than 25 dB-Hz (based on calculations at X-band provided in [1]). Thus, in the following we consider the non-coherent BFSK demodulator. The general architecture is depicted in Fig. 2.

As indicated in Fig. 2, the input baseband data first are spectrum analyzed to obtain an estimate of the carrier frequency F_{init} (frequency of spectrum peak), which is used to initialize the frequency sweep acquisition algorithm. The sweep acquisition is driven by the in-phase component (I) of the de-rotated input and typically starts at $F_{init} - 100$ Hz. The quadrature component (Q), on the other hand, forms the error signal that feeds the carrier-tracking phase-locked loop (PLL) filter as well as the BFSK detector, which is described in Section III.A.

Note that the input to the semaphore demodulator will depend on the receiver front-end that is used to capture the transmitted tones. In the following, we consider two different types of demodulator input data: (1) complex baseband data at a nominal rate of 75 kHz, as produced by the Electra receiver front-end, for example, for the Mars Reconnaissance Orbiter (MRO) record mode and (2) real, 1-bit canister baseband data, as used, for example, in the Mars Odyssey mission.

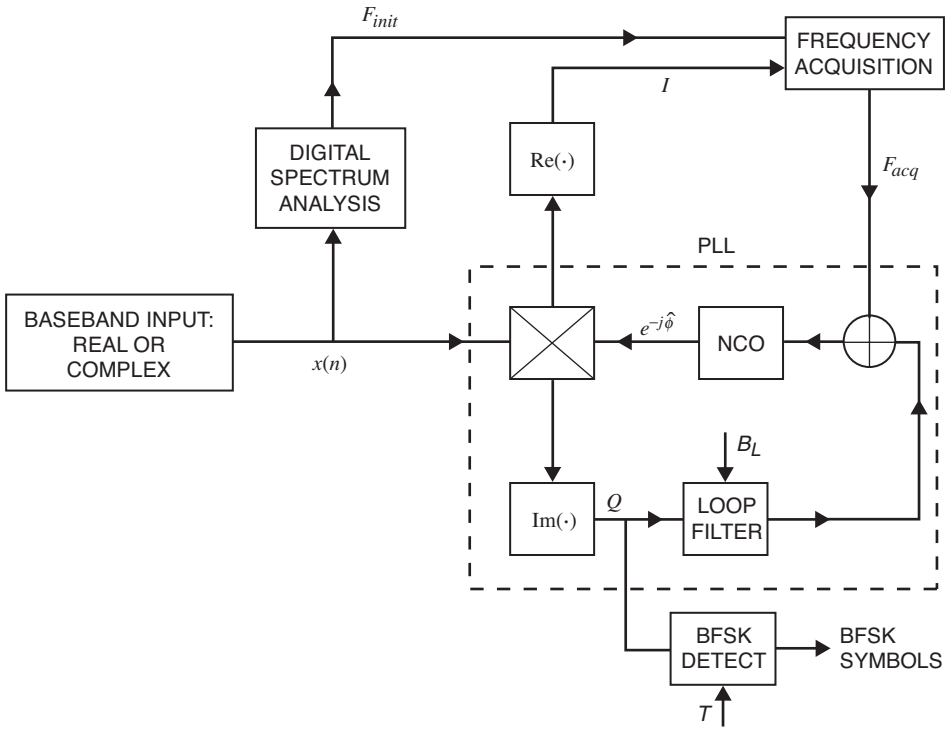

Fig. 2. Semaphore demodulation architecture.

A. Complex Baseband Data Demodulation

The complex baseband equivalent of Eq. (1) is given by

$$z(t) = \sqrt{P} \cdot \exp\left\{j(\delta \cdot s(t) + 2\pi\Delta f t + \phi_c)\right\} = \sqrt{P} \cdot \left\{\cos\delta + j\sin\delta \cdot s(t)\right\} \cdot e^{j(2\pi\Delta f t + \phi_c)} \tag{5}$$

where Δf represents the difference between the nominal transmitted and received carrier frequencies, due to Doppler offsets or carrier drift, for example. Replacing $s(t)$ in Eq. (2) with its fundamental component, $(4/\pi) \cdot \sin(2\pi t/T_P) = (2/j\pi) \cdot \{\exp(2\pi j t/T_P) - \exp(-2\pi j t/T_P)\}$, we have the following approximation for $z(t)$ over $0 \le t \le T$:

$$z(t) \sim \sqrt{P} \cdot \left\{\cos\delta \cdot e^{j(2\pi\Delta f t + \phi_c)} + \sin\delta \cdot \left(\frac{2}{\pi}\right) \cdot \left(e^{j\left(2\pi(\Delta f + f_p)t + \phi_c\right)} - e^{j\left(2\pi(\Delta f - f_p)t + \phi_c\right)}\right)\right\} \tag{6}$$

where $f_P \equiv 1/T_P$. Thus, aside from the residual carrier, one symbol of the received waveform also comprises two sine-wave components (data-tone sidebands) at the sum and difference frequencies: $\Delta f \pm f_P$.

Complex mixing out of the residual-carrier (assuming perfect carrier tracking) results in the waveform (over $0 \le t \le T$)

$$\hat{z}(t) = z(t) \cdot e^{-j(2\pi\Delta f t + \phi_c)} \sim \sqrt{P} \cdot \left\{\cos\delta + \sin\delta \cdot \left(\frac{2}{\pi}\right) \cdot \left(e^{2\pi j f_p t} - e^{-2\pi j f_p t}\right)\right\} \tag{7}$$

Thus, we now have the residual-carrier component at 0 and the data-tone sidebands at $\pm f_P$—a total of three complex sine-wave components. Furthermore, note that

$$\text{Im}\,\{\hat{z}(t)\} \sim 2\sqrt{P}\cdot\sin\delta\cdot\left(\frac{2}{\pi}\right)\cdot\sin(2\pi f_p t) \tag{8}$$

This now becomes the usual, real BFSK detection problem, with the one-sided noise spectral density N_0 being equivalent to the input complex noise spectral density, and thus $E_b/N_0 = P_s\cdot T/N_0$, where P_s represents the signal power in Eq. (8), i.e., $P_s = 2P\cdot\sin^2\delta\cdot(2/\pi)^2$. Thus, the corresponding E_b/N_0 for BFSK symbol detection is given by

$$\frac{E_b}{N_0} = \frac{P\cdot T}{N_0}\cdot\left(\sqrt{2}\cdot\sin\delta\cdot\frac{2}{\pi}\right)^2 \tag{9}$$

At the nominal 60-deg modulation index, we have $20\log_{10}\left(\sqrt{2}\cdot\sin\delta\cdot 2/\pi\right) \sim -2.2$ dB. Given the (theoretical) bit-error rate (BER) for non-coherent BFSK detection, BER $= 0.5\cdot\exp(-0.5E_b/N_0)$ as plotted in Fig. 3, we see that BER $= 10^{-3}$ requires $E_b/N_0 \sim 11$ dB. At 80 bps ($T = 1/80$ s), this corresponds to $P/N_0 = 11 - 20\log_{10}\left(\sqrt{2}\cdot\sin\delta\cdot 2/\pi\right) - 10\log_{10}(T) \sim 32.2$ dB-Hz. The bit-detection statistic for non-coherent BFSK detection Z is:[3]

$$Z = \left|\int_0^T dt\cdot\text{Im}\{\hat{z}(t)\}\cdot\exp(-2\pi j f_p t)\right|^2 + \left|\int_0^T dt\cdot\text{Im}\{\hat{z}(t)\}\cdot\exp(2\pi j f_p t)\right|^2 \tag{10}$$

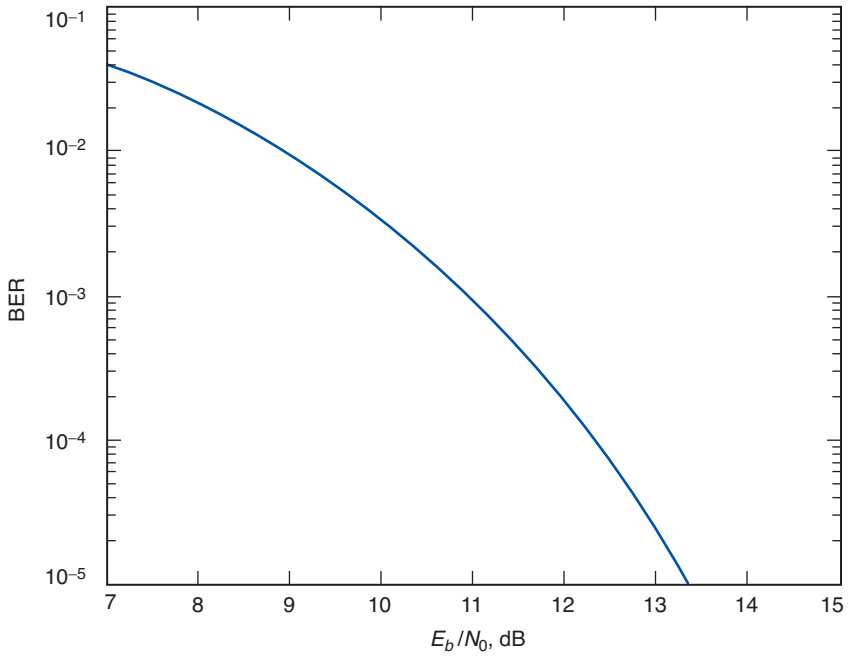

Fig. 3. Ideal noncoherent BFSK BER performance.

[3] Note that we can in principle achieve a further reduction in received signal threshold by using coherent BFSK detection (especially since we are already using a PLL to track out the carrier). However, the non-coherent detector is more robust, e.g., in the case when there are not an integral number of semaphore periods per BFSK symbol interval.

B. Canister Data Demodulation

Returning to Eq. (1) but assuming that the input has been mixed down to Δf as defined in Eq. (5), and again replacing $s(t)$ with its fundamental component, $(4/\pi) \cdot \sin(2\pi t/T_P)$, we have the following approximation for $x(t)$ over $0 \le t \le T$:

$$x(t) \sim \sqrt{2P} \cdot \left\{ \cos\delta \cdot \cos(2\pi\Delta f t + \phi_c) - \sin\delta \cdot \left(\frac{4}{\pi}\right) \cdot \sin(2\pi t/T_p) \cdot \sin(2\pi\Delta f t + \phi_c) \right\}$$

$$= \sqrt{2P}$$

$$\cdot \left\{ \cos\delta \cdot \cos(2\pi\Delta f t + \phi_c) - \sin\delta \cdot \left(\frac{2}{\pi}\right) \cdot (\cos(2\pi(\Delta f - f_p)t + \phi_c) - \cos(2\pi(\Delta f + f_p)t + \phi_c)) \right\} \tag{11}$$

Thus, aside from the residual carrier, with received power $P \cdot \cos^2\delta$, one symbol of the received waveform also comprises two sine-wave components at the sum and difference frequencies: $\Delta f \pm f_P$. The combined power in these two sine-wave components is $2P \cdot \sin^2\delta \cdot (2/\pi)^2$, which is about 61 percent of the total received power when $\delta = \pi/3$, in agreement with Eq. (4).

Complex mixing out of the residual carrier results in the waveform (over $0 \le t \le T$)

$$z(t) = x(t) \cdot e^{-j(2\pi\Delta f t + \phi_c)}$$

$$\sim \sqrt{2P} \cdot \left(\frac{1}{2}\right) \left\{ \cos\delta \cdot \left(1 + e^{-j(4\pi j\Delta f t + 2\phi_c)}\right) - \sin\delta \cdot \left(\frac{2}{\pi}\right) \right.$$

$$\left. \cdot \left(e^{-j\{2\pi(2\Delta f - f_p)t + 2\phi_c\}} + e^{-2\pi j f_p t} - e^{2\pi j f_p t} - e^{-j\{2\pi(2\Delta f + f_p)t + 2\phi_c\}}\right) \right\} \tag{12}$$

Thus, now we have the residual-carrier components at 0 and $-2\Delta f$ as well as components at $\pm f_P - 2\Delta f$ and at $\pm f_p$—a total of six complex sine-wave components (in contrast to complex basebanding, in which case there are only three components). In this case,

$$\mathrm{Im}\{z(t)\} \sim \sqrt{\frac{P}{2}} \cdot \left\{ -\cos\delta \cdot \sin(4\pi\Delta f t + 2\phi_c) + \sin\delta \right.$$

$$\left. \cdot \left(\frac{2}{\pi}\right) \cdot \left(2\sin(2\pi f_p t) - 2\sin(2\pi f_p t) \cdot \cos(4\pi\Delta f t + 2\phi_c)\right) \right\} \tag{13}$$

Again, this is a real BFSK detection problem, but with the one-sided noise spectral density N_0 being equivalent to one-half the input one-sided noise spectral density (by virtue of the $\mathrm{Im}\{\cdot\}$ operation), and thus $E_b/N_0 = 2P_s \cdot T/N_0$, where P_s represents the signal power in Eq. (13),[4] i.e., $P_s = P \cdot \sin^2\delta \cdot$

[4] Here we are ignoring the components in Eq. (13) that are modulated by $\cos(4\pi\Delta f t + 2\phi_c)$ and $\sin(4\pi\Delta f t + 2\phi_c)$. These are treated as interference components and will be approximately removed by the BFSK detector except at certain offset frequencies Δf, as subsequently noted.

$(2/\pi)^2$. Thus, the corresponding E_b/N_0 for BFSK symbol detection is again given by Eq. (9), resulting in the same thresholds (e.g., a 10^{-3} BER threshold of $P/N_0 \sim 32.2$ dB-Hz at 80 bps). However, with 1-bit quantization, we lose another $10\log_{10}(2/\pi) \sim 2$ dB, and thus the BER $= 10^{-3}$ threshold for BFSK canister data at 80 bps is about 34.2 dB-Hz or a signal threshold of -135.8 dBm (assuming a -170-dBm/Hz receiver noise spectral density).

One final point is that with canister data the BFSK detection breaks down at specific Doppler offset frequencies Δf for which some of the various line frequencies at $2\Delta f$ and $2\Delta f \pm f_P$ coincide with the BFSK frequencies $\pm f_p$. So, for example, if $\Delta f = 2$ kHz, then the residual-carrier component at $-2\Delta f$ interferes with the -4-kHz BFSK tone, and the line component at $f_P - 2\Delta f$ would interfere with the $+4$-kHz BFSK tone when $f_P = 8$ kHz (similarly, the line component at $-f_P - 2\Delta f$ would interfere with the -8-kHz BFSK tone when $f_P = 4$ kHz). However, these anomalies would create only BER degradations, e.g., when the difference between Δf and 2 kHz is on the order of $1/T$, and thus this typically would present only a brief degradation of BER performance over time. Examples of these anomalies are presented in Section IV. Note that they are not present with complex basebanding.

IV. Performance Results

Various simulations have been carried out demonstrating semaphore demodulation performance for both complex and canister input data types. As an illustrative example, we have computed BERs under the assumption of perfect residual-carrier tracking and with $T = 1/80$ s. The results are presented in Fig. 4 for near the measured 10^{-3} BER threshold (~34.2 dB-Hz for canister input data and ~32.2 dB-Hz for complex input data—note that these are in agreement with the results provided in Section III). The 2-dB hard-limiting loss for the canister input data is clearly observed. Note also the large loss in performance with the canister input as the carrier frequency offset Δf approaches 2 kHz, as predicted in Section III.

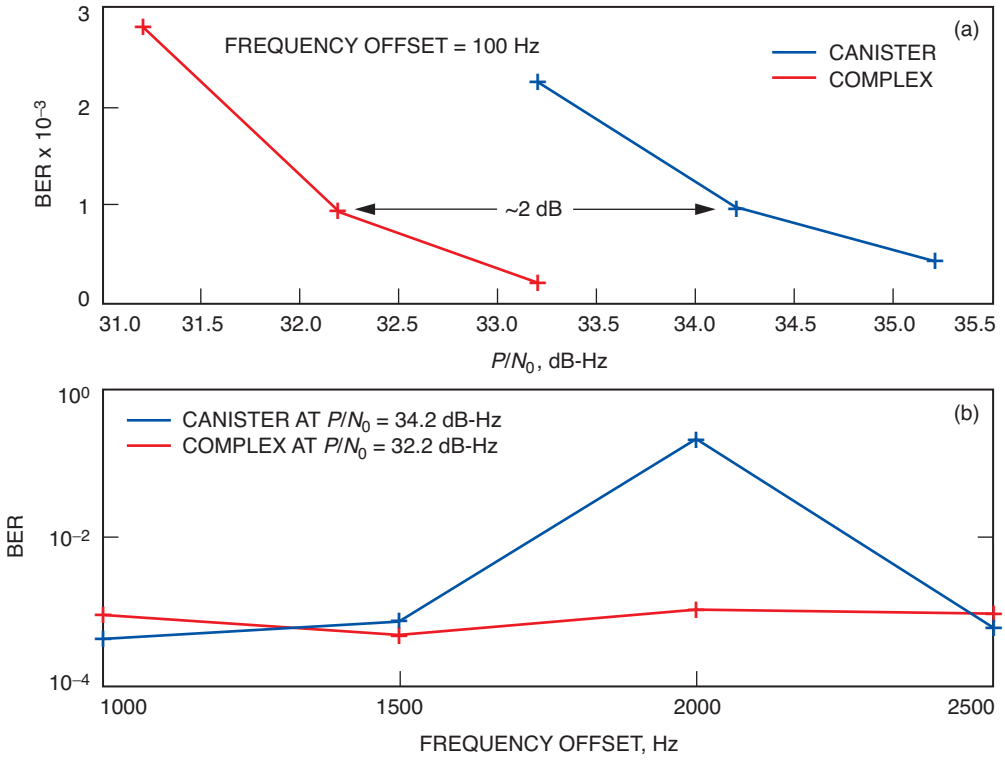

Fig. 4. Simulated BER performance: (a) BER versus P/N_0 and (b) BER versus frequency offset.

We have carried out simulations with a time-varying carrier offset frequency (also assuming perfect residual-carrier tracking). An interesting example is when the carrier offset is (linearly) swept through one of the regions of frequency ambiguity for the canister input data case. In particular, we consider a frequency profile linearly varying between 1850 and 2150 Hz over a span of 12.5 s (corresponding to 1000 BFSK symbols with $T = 1/80$ s). For the canister input, we used a constant $P/N_0 = 34.2$ dB-Hz, whereas for the complex input case, $P/N_0 = 32.2$ dB-Hz. The measured BER for the complex input was 1 error over the 1000 BFSK symbols, whereas for the canister input 12 symbol errors were observed, reflecting the 2-kHz frequency crossover. It is also of interest in this case to examine the canister and complex input spectra. These are presented in Figs. 5(a) and 5(b). Referring first to the canister input spectrogram, Fig. 5(a), various spectral components are observed relating to the carrier and data tone components as well as spurious harmonics generated by the 1-bit sampling. The linear meandering of the carrier also is clearly observed. In contrast, the complex input spectrogram, Fig. 5(b), is much cleaner with only 3 dominant spectral components, as described in Section III.

Finally, we have analyzed canister data collected from the CE505 radio. The radio was programmed to generate semaphores at either 8 or 80 BFSK symbols/s. Three successive spectral snapshots (at 80 symbols/s) are presented in Fig. 6, showing the transition from a 0-symbol (4-kHz data tone frequency) to a 1-symbol (8-kHz data tone frequency). Three data files were demodulated with the semaphore demodulator depicted in Fig. 2: (1) 80-symbols/s data at approximately a −125-dBm input signal level (corresponding to $P/N_0 \sim 45$ dB-Hz); (2) 80-symbols/s data at approximately a −130-dBm input signal level (corresponding to $P/N_0 \sim 40$ dB-Hz); and (3) 8-symbols/s data at approximately a −140-dBm input signal level (corresponding to $P/N_0 \sim 30$ dB-Hz). In all cases, no symbol errors were detected.

V. Conclusions

In this article, a simple form of binary frequency-shift keying has been devised that can be transmitted simply by appropriately programming the input bit stream to the residual-carrier, BPSK modulator. Furthermore, this approach is not restricted in synthesized data rates, thus making it a perfect backup for stressing link conditions such as during EDL. Performance estimates for this approach were presented, and various data analysis results were provided for both synthesized and actual measured laboratory data.

References

[1] E. Satorius, P. Estabrook, J. Wilson, and D. Fort, "Direct-to-Earth Communications and Signal Processing for Mars Exploration Rover Entry, Descent, and Landing," *The Interplanetary Network Progress Report 42-153, January–March 2003*, Jet Propulsion Laboratory, Pasadena, California, pp. 1–35, May 15, 2003. http://ipnpr.jpl.nasa.gov/tmo/progress_report/42-153/153A.pdf

[2] G. E. Wood, S. W. Asmar, T. A. Rebold, and R. A. Lee, "Mars Pathfinder Entry, Descent, and Landing Communications," *The Telecommunications and Data Acquisition Progress Report 42-131, July–September 1997*, Jet Propulsion Laboratory, Pasadena, California, pp. 1–19, November 15, 1997. http://tmo.jpl.nasa.gov/tmo/progress_report/42-131/131I.pdf

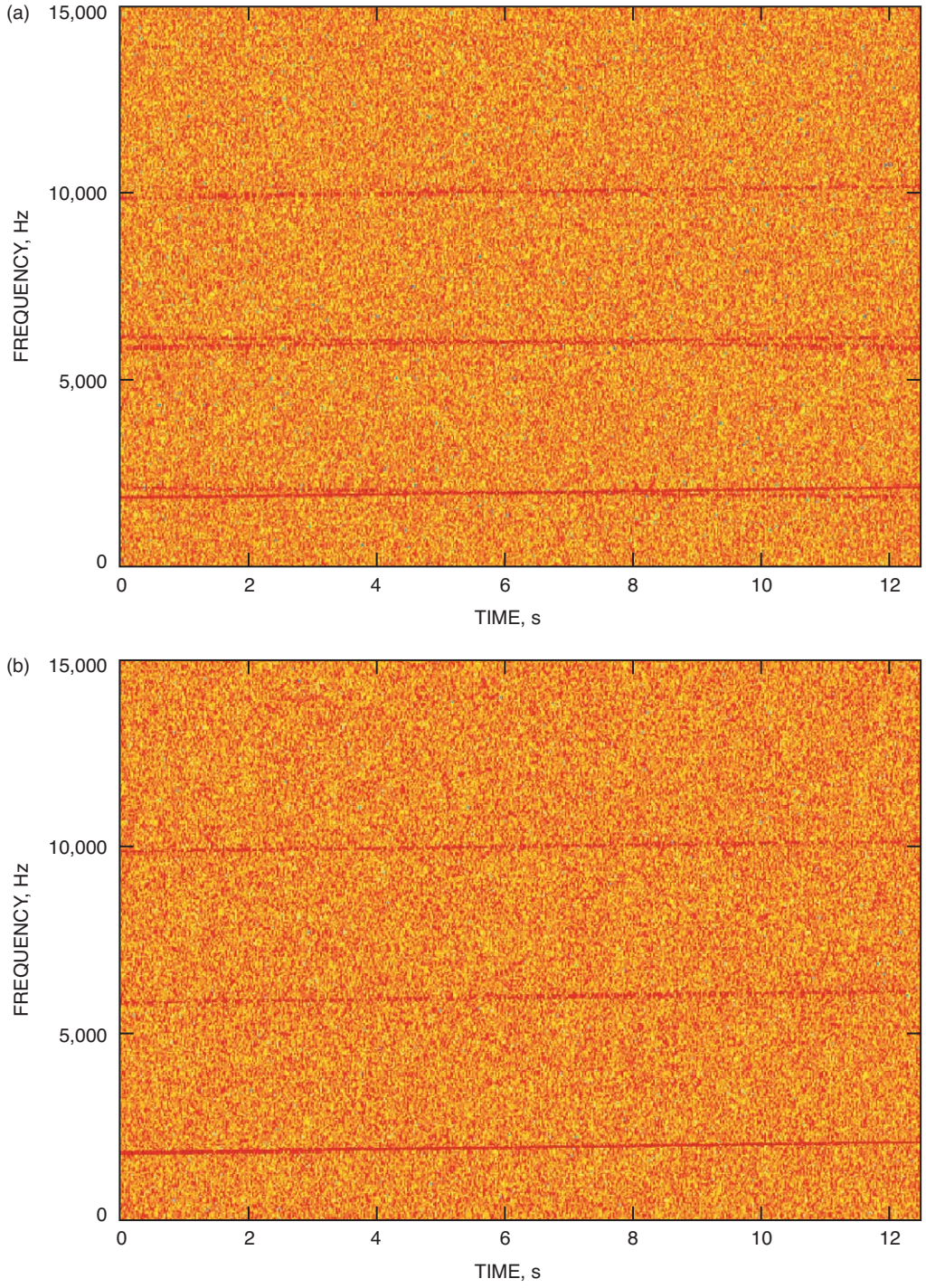

Fig. 5. Input spectrograms: (a) canister and (b) complex.

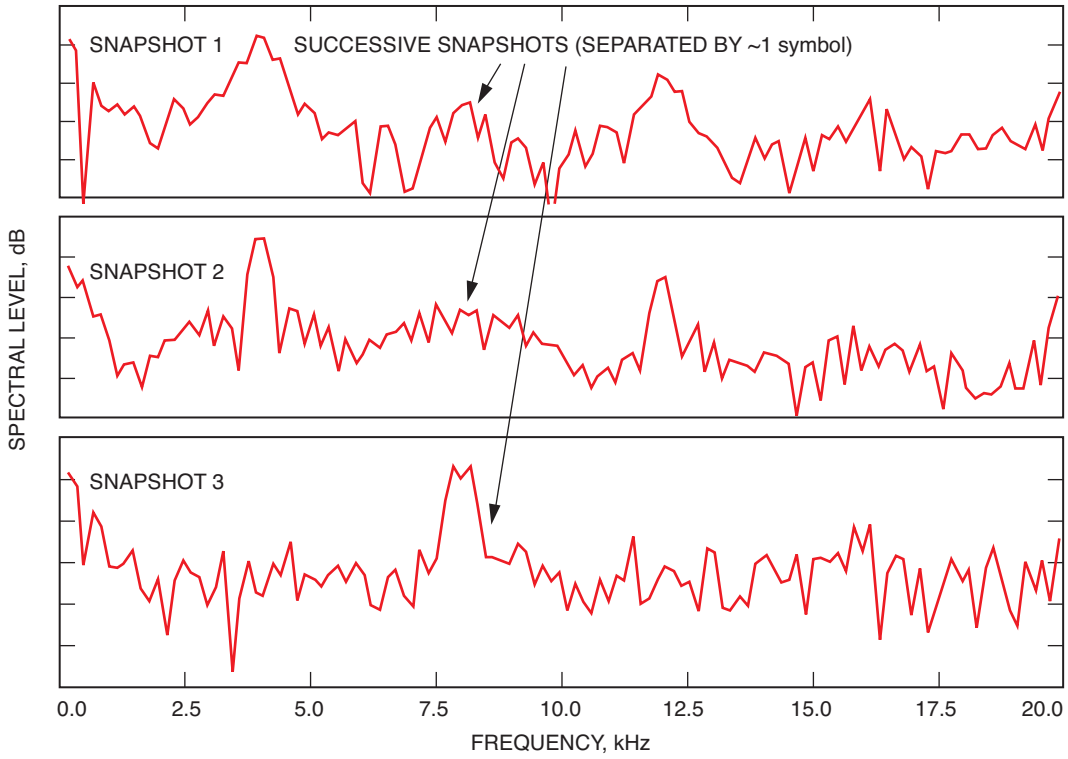

Fig. 6. Spectral snapshots from CE505 recorded canister data.